DOI: 10.15825/1995-1191-2025-2-163-170

LYMPHOCYTIC RNA STIMULATES PHYSIOLOGICAL REGENERATION AND ENHANCES MICROCIRCULATION IN THE THYROID GLAND

N.V. Tishevskaya, E.S. Golovneva, R.V. Takhaviev
South Ural State Medical University, Chelyabinsk, Russian Federation

Objective: to investigate the regulatory effects of exogenous lymphocyte RNA on thyroid gland regeneration. **Materials and methods.** The study was conducted on 18 male Wistar rats (310–350 g), divided into three groups (n = 6 per group). Group 1 – intact rats; group 2 – control rats (subjected to 6 weeks of physical activity), group 3 – experimental rats (subjected to 6 weeks of physical activity + RNA injection). Total RNA, isolated from the spleen of a 30-day-old pig, was administered four times at a dose of 30 μg/100 g body weight, once per week. Follicular epithelium and vascular structures were analyzed using morphometry, VEGF content was quantified via immunohistochemistry with specific antibodies, and thyroid microvascular function was assessed using laser flowmetry. **Results.** Following RNA administration, the relative thyroid gland mass increased by 16%, the follicular epithelium area expanded 1.5-fold, and the vasculature area doubled. Additionally, VEGF content increased 2.5-fold compared to intact rats, while microcirculation intensity rose by 64%, and vascular resistance decreased by 21%. **Conclusion.** Administration of morphogenetically active total RNA under conditions of increased oxygen demand promotes regenerative hypertrophy of the glandular epithelium and enhances microcirculation in the thyroid gland.

Keywords: RNA, regeneration, microcirculation, thyroid gland.

INTRODUCTION

Regenerative thyroidology focuses on the ability of thyroid tissue to renew itself and recover after injury or resection, and experimental evidence demonstrating the induction of thyrocyte proliferation and differentiation *in vitro*. However, the underlying mechanisms of thyroid regeneration remain poorly understood. In murine models, a distinct cluster of cells expressing the transcription factor NKX2-1 – a key regulator of thyroid growth, development, and functional maintenance – has been identified within the thyroid gland [1]. These NKX2-1-positive cells are assumed to represent precursor populations that, through differentiation and maturation, give rise to the follicular architecture of the thyroid [2]. Notably, thyroid tissue retains a lifelong potential for hypertrophic and hyperplastic regeneration, a process that may be activated in response to increased thyroid-stimulating hormone secretion from the adenohypophysis during physiological stress or intense physical activity [3, 4]. During physical activity, the body enters a distinct hormonal state in which the thyroid gland enhances the secretion and release of thyroxine and triiodothyronine into the bloodstream. This increased hormonal output leads to a reduction in the colloid content within thyroid follicles. It has been shown that after a single session of intensive physical exercise, there is a rapid decrease in follicle size. Moreover, with sustained daily physical training over a 35-day period, adaptive and compensatory responses are reinitiated within the thyroid gland. These changes are characterized by a marked increase in the proliferative activity of the thyroid epithelium [5].

In mammals, tissue growth and development are regulated, in part, by tissue-specific clones of T-lymphocytes. Early studies identified T cells within the lymph nodes of Wistar rats that began to proliferate robustly upon contact with thyrocytes or after addition of rat thyroglobulin to the culture medium [6]. Cloning of these thyroid-specific T-lymphocytes revealed that all clones exhibited a $CD4^+CD8^-$ phenotype. Of the 23 T-cell clones analyzed, 7 showed selective proliferation in the presence of thyrocytes alone, while the remainder proliferated in response to both thyrocytes and thymic cells [7]. Further investigations of T-lymphocytes isolated directly from the thyroid gland identified the presence of both $CD4^+$ T-helper cells and $CD8^+$ cytotoxic T cells, all expressing αβ T-cell receptors [8]. $CD4^+$ T-helper cells were found to localize predominantly in the centers of thyroid lymphoid follicles, whereas $CD8^+$ T cells were primarily distributed along the follicular periphery [9]. Under physiological conditions, both $CD4^+$ T-helper cells and cytotoxic T lymphocytes contribute to thyrocyte hyperplasia and proliferation through production of tumor necrosis factor-alpha (TNF-α). In experimental models, mice lacking T-helper cells exhibited signs of thyroid

Corresponding author: Natalya Tishevskaya. Address: 64, Vorovskogo str., Chelyabinsk, 454092, Russian Federation. Phone: (351) 232-74-67. E-mail: natalya-tishevskaya@yandex.ru

fibrosis when exposed to the activity of cytotoxic T lymphocytes alone [10].

To date, compelling evidence has shown that not only lymphoid cells themselves, but also total RNA isolated from these cells, can stimulate tissue regeneration and enhance cell–cell interactions in rapidly renewing tissues. For example, erythroid cells and bone marrow macrophages are known to actively form new erythroblastic islets, not only in response to erythropoietin and macrophage colony-stimulating factor [11], but also following the administration of exogenous lymphocytic RNA in experimental animals [12]. Based on this, the present study aimed to explore the regulatory role of morphogenetically active exogenous RNA on cellular processes in a slowly renewing secretory organ – the thyroid gland – under conditions of enhanced tissue respiration induced by regular physical exercise.

MATERIALS AND METHODS

The study was conducted on 18 male Wistar rats weighing 310–350 g. All experimental procedures adhered to the principles of humane treatment outlined in the European Union Directive 86/609/EEC, the Declaration of Helsinki, and the Order of the Ministry of Health of the Russian Federation No. 199N dated April 1, 2016, "On the Approval of the Rules of Good Laboratory Practice". Animals were housed in standard cages (n = 6 per cage) with ad libitum access to food and water, maintained at an ambient temperature of +24 ± 2 °C in accordance with sanitary regulations SP 2.2.1.3218.

The animals received a daily diet of specialized pelleted feed that met international standards for nutrient, vitamin, and mineral content, in accordance with GOST R 50258-92 ("Complete feeds for laboratory animals"). All procedures involving potential pain or distress were performed under general anesthesia, and euthanasia was carried out in a designated room, separate from the animal housing area, using ether anesthesia followed by cervical dislocation.

The experimental animals were randomly divided into 3 groups, with 6 rats per group: Group 1 consisted of intact (non-exercised, untreated) rats; Group 2 included control rats subjected to a 6-week exercise protocol; Group 3 consisted of rats undergoing the same 6-week exercise regimen and receiving additional injections of total RNA.

The training regimen involved swimming exercises performed in a 200-liter tank filled with water to a depth of 0.5 meters, maintained at a temperature of +22–23 °C. The rats swam 3 times per week, with the duration of each session gradually increasing from 30 minutes to 55 minutes, in 5-minute increments each week.

Lymphocytes, the source of morphogenetically active RNA, were isolated from the spleen of a 30-day-old piglet. The tissue was homogenized in a glass homogenizer, filtered through a capron mesh, and subjected to 3 rounds of centrifugation in sterile 0.9% NaCl solution to collect the cells. Total RNA was extracted using the guanidine thiocyanate–phenol–chloroform method. RNA concentration was determined spectrophotometrically by measuring optical density at 260 nm. The extracted RNA was lyophilized and stored in sterile vials at +5 °C. Stability tests confirmed that the RNA quantity remained unchanged after lyophilization.

Before injection, lyophilized RNA was dissolved in sterile 0.9% NaCl, filtered using sterile syringe filters with a pore size of 0.22 μm, and administered intraperitoneally. Each rat in Group 3 received a total of four injections, administered once weekly, at a dose of 30 μg RNA per 100 g body weight in a total volume of 0.5 mL per injection.

Six weeks after the start of the experiment, the microcirculatory status of the thyroid gland was assessed in all animals using laser Doppler flowmetry with the LAKK-OP analyzer (NPO "LAZMA", Russia). The procedure was performed under general anesthesia (Zoletil, 10 mg/kg, intramuscularly; VIRBAC, France). After careful dissection of the skin and adjacent tissues, the device's sensor was placed directly on the thyroid tissue and securely fixed to the lateral skin margins using adhesive tape.

The Doppler flowmetry data were analyzed using proprietary software from NPO "LAZMA", focusing on the following parameters: microcirculation Index – the arithmetic mean value of perfusion, expressed in perfusion units (p.u.); shunt coefficient (Sc) calculated as: Sc = An/Am, where An – is the largest amplitude of perfusion fluctuations in the neurogenic range (p.u.), Am – is the largest amplitude of perfusion fluctuations in the myogenic range (p.u.); the resistance coefficient of the microcirculatory channel was calculated using the formula: Rc = (AHF + ACF)/σ where is the amplitude of fast (respiratory) fluxmotion waves (p.u.), ACF is the amplitude of cardiac (pulse) fluxmotion waves (p.u.), σ is the standard deviation of the amplitude of blood flow fluctuations from the mean microcirculation index. The amplitude-frequency spectra of perfusion oscillations were assessed within specific frequency ranges:

- Endothelial oscillations (A(E)): 0.007–0.017 Hz
- Neurogenic oscillations (A(H)): 0.023–0.046 Hz
- Myogenic oscillations (A(M)): 0.06–0.15 Hz
- Respiratory rhythm (A(D)): 0.21–0.6 Hz
- Cardiac rhythm (A(C)): 0.7–1.6 Hz

The amplitudes were then normalized to the standard deviation (σ) and mean microcirculation index (M), enabling the assessment of the functional contribution of each regulatory mechanism to modulation of microcirculatory flow. The following normalized parameters were calculated:

- Endothelial activity (E) = A(E)/3σ
- Neurogenic activity (H) = A(H)/3σ
- Myogenic activity (M) = A(M)/3σ
- Respiratory rhythm (D) = A(D)/3σ

– Cardiac rhythm (C) = A(C)/3σ

These normalized parameters were automatically computed by the system after identifying the maximum amplitude (Amax) within the corresponding frequency range [13].

After measurement of microcirculation parameters, the animals were euthanized. Thyroid tissue samples were fixed in 10% neutral buffered formalin. Standard histological processing was performed, including paraffin embedding, sectioning, and staining with hematoxylin and eosin.

Histological evaluation was conducted using a LEICA DMRXA microscope (Germany) equipped with a LEICA DFC 290 digital video camera and connected to a personal computer. Microstructural images were captured in *TIFF format within the RGB color space. Quantitative analysis was performed using the licensed ImageScope-M image analysis software (Russia), measuring the following parameters: total follicle area, follicular and vascular lumen area, thyrocyte nuclear area, epithelial height, and vascular wall thickness. The relative vascular area was calculated as the percentage ratio of vessel area to total tissue section area.

Vascular endothelial growth factor (VEGF) expression was assessed immunohistochemically using specific anti-VEGF antibodies (Biorbyt, USA) and a biotin-streptavidin-peroxidase detection system (DakoCytomation, Denmark). Integral VEGF index was calculated as the product of the stained area (relative) and staining intensity (scored), with results expressed in arbitrary units.

Data were analyzed using licensed versions of Microsoft Excel 2020 and PAST software (version 4.03). The nonparametric Mann–Whitney U test was applied to evaluate significance of differences between groups. Comparative analysis of morphometric data sets was performed using Wald's sequential probability ratio test [14]. Results are presented as arithmetic mean ± standard error of mean (M ± m). A p-value of ≤0.05 was considered statistically significant.

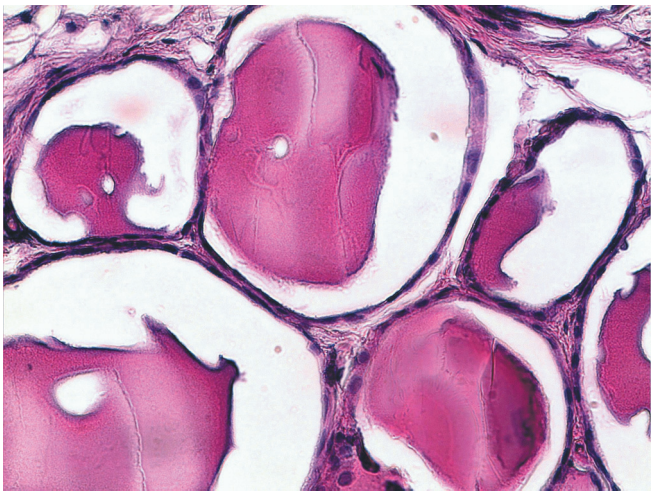

Fig. 1. Follicular apparatus of the thyroid gland. Group 1 (intact rats). H&E stain; 400×; oil immersion

RESULTS

Histological analysis of thyroid tissue in rats from Group 2 (Fig. 2), which underwent regular physical exercise, revealed a reduction in follicle size, decreased colloid content, and morphological changes in the follicular epithelium, which adopted a cuboidal shape compared to the intact animals (Fig. 1). In Group 3 animals, which were exposed to the same physical exercise regimen but also received total RNA (Fig. 3), a similar decrease in follicle size and colloid volume was observed. However, the follicular epithelium exhibited a highly prismatic structure with pronounced papillary proliferation. This histological pattern is recognized as indicative of enhanced hormone-producing activity of the thyroid gland [15]. These findings suggest that total RNA administration enhanced the functional activity

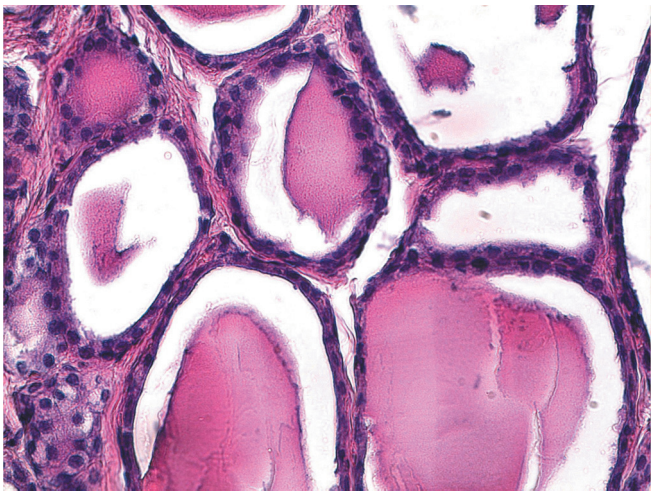

Fig. 2. Follicular apparatus of the thyroid gland. Group 2 (physical activity). H&E stain; 400×; oil immersion

Fig. 3. Follicular apparatus of the thyroid gland. Group 3 (physical activity + RNA). H&E stain; 400×; oil immersion

of the glandular epithelium, thereby supporting an adequate supply of thyroid hormones required to meet the increased physiological demands associated with regular physical exertion.

Morphometric analysis revealed that, in the control group rats subjected to several days of physical activity, thyroid gland mass did not differ significantly from that of intact animals (Table 1). However, in rats exposed to the same physical activity regimen but additionally administered lymphocytic RNA, both the absolute and relative mass of the thyroid gland were increased compared to the intact group. Specifically, the relative gland mass in group 3 was 16.7% higher than in group 1 and 15% higher than in group 2. A marked and statistically significant increase in the area occupied by follicular epithelium cells was also observed in group 3 – 1.5 times greater than in intact animals and 1.4 times greater than in the control group. These structural alterations were corroborated by morphometric findings: epithelial cell height in group 3 animals was 33% greater, while the follicular cavity area was 39% less compared to intact rats.

Morphometric analysis of arterioles and venules in the thyroid tissue revealed a pronounced reorganization of the microcirculatory bed in response to exogenous RNA administration. In group 3 animals, a significant increase in the thickness of arteriole and venule walls was observed compared to both intact rats and the control group. Additionally, the relative area of the vascular bed was doubled. This expansion of the microcirculatory network likely resulted from the formation of new capillaries, as the luminal area of arterioles and venules remained unchanged. Supporting the evidence of angiogenic activation, a marked elevation in VEGF content was detected in the thyroid tissue gland of animals subjected to prolonged physical exercise. While VEGF levels in group 2 animals increased by 1.9-fold relative to intact controls, group 3 rats, which received exogenous RNA in conjunction with regular physical activity, exhibited a 2.5-fold increase in VEGF content.

Previous studies have demonstrated that the angioprotective effects of lymphoid cells may be attributed to their elevated expression of hypoxia-inducible factor 1-alpha (HIF-1α), a key regulator that promotes VEGF synthesis under hypoxic conditions [16]. A dual role of T-lymphocytes in regulating angiogenesis and cell proliferation has been documented in renal tissue [17]. It was shown that T-lymphocytes migrating to areas of tissue injury exerted a pronounced proangiogenic and proregenerative effect during reparative regeneration. Conversely, in conditions leading to fibrosis, their role shifted toward a predominantly proinflammatory profile. These findings highlight the remarkable functional plasticity of T-cells in morphogenetic processes, a capacity that remains both underrecognized and poorly explored in the context of tissue regeneration.

Using laser Doppler flowmetry combined with spectral amplitude-frequency wavelet analysis of blood flow oscillations in microvessels, we assessed the functional changes in the thyroid microcirculatory bed induced by morphogenetically active exogenous RNA (Table 2). Regular physical activity in rats of group 2 led to a 38% increase in the microcirculation index compared to intact controls. Notably, administration of exogenous RNA in rats subjected to identical physical exertion (group 3) resulted in a 64% increase in this index. The vascular shunt coefficient within the microcirculatory network remained stable across groups. However, a 21% decrease in the resistance coefficient was observed in group 3 animals, indicating improved vascular wall elasticity. This suggests optimal blood supply to the follicular apparatus of the thyroid gland in animals that received total RNA.

Changes in the normalized parameters of amplitude-spectral analysis (Fig. 4) further indicated enhanced engagement of both local and systemic regulatory me-

Table 1

Thyroid morphometry

Indicators	Intact rats (group 1), n = 6	Physical activity (Swimming)	
		Control (group 2), n = 6	RNA injection (group 3), n = 6
Absolute thyroid mass (g)	0.245 ± 0.009	0.255 ± 0.009	0.286 ± 0.012*
Relative thyroid mass (μg/g)	0.74 ± 0.03	0.75 ± 0.05	0.86 ± 0.04*▲
Follicular epithelium area (μm^2)	1242.1 ± 56.6	1358.4 ± 44.3	1871.7 ± 40.5*▲
Follicular epithelium height (μm)	7.6 ± 0.4	8.9 ± 0.6	10.1 ± 0.3*▲
Follicle cavity area (μm^2)	3645.5 ± 99.8	3162.2 ± 31.4*	2236 ± 22.2*▲
Thyrocyte nuclei area (μm^2)	13.2 ± 0.7	13.1 ± 0.6	12.7 ± 0.7
Arteriole wall thickness (μm)	7.6 ± 0.3	7.9 ± 0.3	8.7 ± 0.3*▲
Arteriole lumen area (μm^2)	121.3 ± 18.8	123.3 ± 14.6	127.8 ± 16.2
Venule wall thickness (μm)	4.2 ± 0.1	4.4 ± 0.3	5.1 ± 0.2*
Venule lumen area (μm^2)	218.2 ± 16.5	193.2 ± 13.7	191.9 ± 11.9
Relative vasculature area (%)	4.2 ± 0.2	4.8 ± 0.3	8.4 ± 0.2*▲
Vascular endothelial growth factor (c.u.)	4.7 ± 0.2	8.9 ± 0.2*	11.9 ± 0.5*▲

Notes: * – differences between groups 2, 3 and group 1 ($p < 0.05$); ▲ – differences between group 2 and group 3 ($p < 0.05$).

chanisms in the thyroid microvasculature of rats that received exogenous RNA. It is well established that rhythmic variability of microvascular blood flow is influenced by several active regulatory components – myogenic (M), neurogenic (N), and endothelial (E) – as well as passive components associated with cardiac (C) and respiratory (D) rhythms. The spectral characteristics of these oscillatory processes not only permitted quantification of the contribution of each of the regulatory mechanisms but also allowed identification of specific features in the adaptive responses of the thyroid microcirculatory network. Notably, during physical exercise, the myogenic component remained largely unchanged, suggesting a stable muscle tone in thyroid precapillaries, which play a critical role in modulating nutrient blood flow. At the same time, the endothelial component – reflecting the influence of vasodilatory substances such as nitric oxide, ADP, and VEGF, as well as passive effects from respiratory and pulse wave modulation – was significantly elevated in the thyroid microcirculatory bed following prolonged physical exercise. In animals that underwent physical activity and received injections of morphogenetically active RNA (group 3), the endothelial component was four times higher than in the control group. Additionally, the cardiac and respiratory components were elevated by twofold and threefold, respectively, compared to rats in the control group.

It is known that stable adaptation and maintenance of structural and hemodynamic homeostasis in microvascular networks at a new functional level are achieved through the coordinated and balanced involvement of all regulatory mechanisms. This is characterized by a uniform increase in amplitude parameters without the dominance of oscillations in any frequency range [18, 19]. Such a regulatory pattern is referred to as multichannel or multistable regulation. In the present study, exogenous RNA administration in combination with regular physical activity resulted in the development of a clearly defined multistable variant of microvascular blood flow regulation.

Table 2

Amplitude-spectral analysis of the thyroid microvasculature (standard indicators)

Indicators	Intact rats (group 1), n = 6	Physical activity (Swimming)	
		Control (group 2), n = 6	RNA injection (group 3), n = 6
Microcirculation index (p.u.)	14.3 ± 0.9	19.8 ± 0.7*	23.5 ± 0.3*▲
Shunt coefficient in the microvasculature (c.u.)	0.87 ± 0.04	1.0 ± 0.04	1.05 ± 0.12
Microcirculatory resistance coefficient (c.u.)	0.88 ± 0.01	0.9 ± 0.01	0.69 ± 0.02*▲

Notes: * – differences between groups 2, 3 and group 1 ($p < 0.05$); ▲ – differences between group 2 and group 3 ($p < 0.05$).

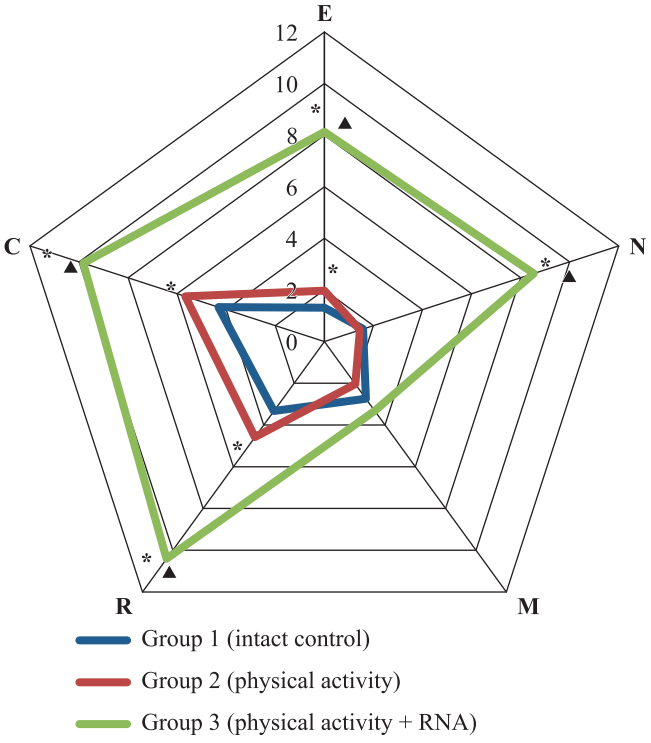

Fig. 4. Amplitude-spectral analysis of the thyroid microvasculature (normalized indicators): endothelial component (E), neurogenic component (N), myogenic component (M), respiratory component (R), cardiac component (C). * – differences between groups 2, 3 and group 1 ($p < 0.05$); ▲ – differences between group 2 and group 3 ($p < 0.05$)

CONCLUSION

The administration of morphogenetically active total RNA, under conditions of increased oxygen demand, induces regenerative hypertrophy of the thyroid glandular epithelium and enhances microcirculation within the organ. This results in a significant increase in both the absolute and relative mass of the thyroid gland, as well as in the size of thyrocytes, the number of capillaries, and the intensity of blood flow in the microcirculatory channel. Exogenous RNA also leads to marked changes in the regulatory parameters of tissue blood flow in the thyroid gland during periods of intensified functional activity. These changes are associated with a notable reduction in vascular wall stiffness and an improved adaptive capacity of the microcirculatory network in the thyroid gland of rats in group 3.

The authors declare no conflict of interest.

REFERENCES

1. *Kusakabe T, Kawaguchi A, Hoshi N, Kawaguchi R, Hoshi S, Kimura S.* Thyroid-specific enhancer-binding protein/NKX2.1 is required for the maintenance of ordered architecture and function of the differentiated thyroid. *Mol Endocrinol.* 2006 Aug; 20 (8): 1796–1809. doi: 10.1210/me.2005-0327.
2. *Iwadate M, Takizawa Y, Shirai YT, Kimura S.* An *in vivo* model for thyroid regeneration and folliculogenesis. *Lab Invest.* 2018 Sep; 98 (9): 1126–1132. doi: 10.1038/s41374-018-0068-x.
3. *Ozaki T, Matsubara T, Seo D, Okamoto M, Nagashima K, Sasaki Y et al.* Thyroid regeneration: characterization of clear cells after partial thyroidectomy. *Endocrinology.* 2012 May; 153 (5): 2514–2525. doi: 10.1210/en.2011-1365.
4. *Dumont J, Lamy F, Roger P, Maenhaut C.* Physiological and pathological regulation of thyroid cell proliferation and differentiation by thyrotropin and others. *Physiol Rev.* 1992 Jul; 72 (3): 667–697. doi: 10.1152/physrev.1992.72.3.667.
5. *Krishtop VV, Rumyantseva TA, Nikonorova VG.* Peculiarities of thyroid morphology in cerebral hypoperfusion in the complex with short-term exercise in rats with different results in the Morris labyrinth. *Journal of Volgograd State Medical University.* 2021; 78 (2): 103–107. doi: 10.19163/1994-9480-2021-2(78)-103-107.
6. *Kimura H, Davies TF.* Thyroid-specific T cells in the normal Wistar rat. I. Characterization of lymph node T cell reactivity to syngeneic thyroid cells and thyroglobulin. *Clin Immunol Immunopathol.* 1991 Feb; 58 (2): 181–194. doi: 10.1016/0090-1229(91)90135-w.
7. *Kimura H, Davies TF.* Thyroid-specific T cells in the normal Wistar rat. II. T cell clones interact with cloned Wistar rat thyroid cells and provide direct evidence for autoantigen presentation by thyroid epithelial cells. *Clin Immunol Immunopathol.* 1991 Feb; 58 (2): 195–206. doi: 10.1016/0090-1229(91)90136-x.
8. *Sugihara S, Fujiwara H, Shearer GM.* Autoimmune thyroiditis induced in mice depleted of particular T cell subsets. Characterization of thyroiditis-inducing T cell lines and clones derived from thyroid lesions. *J Immunol.* 1993 Jan 15; 150 (2): 683–694.
9. *Zha B, Huang X, Lin J, Liu J, Hou Y, Wu G.* Distribution of lymphocyte subpopulations in thyroid glands of human autoimmune thyroid disease. *J Clin Lab Anal.* 2014 May; 28 (3): 249–254. doi: 10.1002/jcla.21674.
10. *Yu S, Fang Y, Sharav T, Sharp GC, Braley-Mullen H.* CD8+ T cells induce thyroid epithelial cell hyperplasia and fibrosis. *J Immunol.* 2011 Feb 15; 186 (4): 2655–2662. doi: 10.4049/jimmunol.1002884.
11. *Tishevskaya NV, Shevyakov SA, Zakharov YuM.* Vliyaniye eritropoetina i makrofagal'nogo koloniyestimuliruyushchego faktora na proliferativnuyu aktivnost' eritroidnykh kletok v kul'turakh eritroblasticheskikh ostrovkov. *Meditsinskiy akademicheskiy zhurnal.* 2003; 3 (3): 67–72. [In Russ.].
12. *Gevorkyan NM, Tishevskaya NV, Bolotov AA.* Effect of preliminary administration of total RNA of bone marrow cells on the dynamics of erythropoiesis recovery in rats after acute gamma irradiation. *Bull Exp Biol Med*. 2016 Sep; 161 (5): 670–673. [In Russ., English abstract]. doi: 10.1007/s10517-016-3494-z.
13. *Krupatkin AI, Sidorov VV.* Funkcional'naya diagnostika sostoyaniya mikrocirkulyatorno-tkanevyh sistem. Kolebaniya, informaciya, nelinejnost'. Rukovodstvo dlya vrachej. Moscow: URSS, 2016; 496. [In Russ.].
14. *Tishevskaya NV, Bolotov AA, Zakharov YuM.* Matematicheskoye modelirovaniye mezhkletochnykh vzaimodeystviy v kul'ture eritroblasticheskikh ostrovkov. *Meditsinskiy akademicheskiy zhurnal.* 2005; 5 (4): 50–59. [In Russ.].
15. *Kirillov YuB, Chumachenko AP, Aristarkhov VG, Potapov AA, Panteleyev IV.* Rapid morphometric method for assessment of thyroid functional activity. *Problems of Endocrinology.* 1994; 40 (4): 19–21. [In Russ.] doi: 10.14341/probl12135.
16. *Lin Y, Tang Y, Wang F.* The Protective effect of HIF-1α in T lymphocytes on cardiac damage in diabetic mice. *Ann Clin Lab Sci.* 2016 Winter; 46 (1): 32–43.
17. *Do Valle Duraes F, Lafont A, Beibel M, Martin K, Darribat K, Cuttat R et al.* Immune cell landscaping reveals a protective role for regulatory T cells during kidney injury and fibrosis. *JCI Insight.* 2020 Feb 13; 5 (3): e130651. doi: 10.1172/jci.insight.130651.
18. *Hu HF, Hsiu H, Sung CJ, Lee CH.* Combining laser-Doppler flowmetry measurements with spectral analysis to study different microcirculatory effects in human prediabetic and diabetic subjects. *Lasers Med Sci.* 2017 Feb; 32 (2): 327. doi: 10.1007/s10103-016-2117-2.
19. *Sun PC, Kuo CD, Wei SH, Lin HD.* Microvascular reactivity using laser Doppler measurement in type 2 diabetes with subclinical atherosclerosis. *Lasers Med Sci*. 2023 Feb 28; 38 (1): 80. doi: 10.1007/s10103-023-03737-x.

The article was submitted to the journal on 11.10.2024